IOP Publishing Superconductor Science and Technology
Supercond. Sci. Technol. 33 (2020) 034008 (8pp) https://doi.org/10.1088/1361-6668/ab6ec2

Breakthrough in the reduction of oxygen-annealing time for REBCO melt-textured bulks under an oxygen atmosphere containing water vapor

T Motoki[1], Y Yanai[1], K Nunokawa[1], S Gondo[1], S Nakamura[2] and J Shimoyama[1]

[1] Department of Physics and Mathematics, Aoyama Gakuin University, 5-10-1 Fuchinobe, Chuo-ku, Sagamihara, Kanagawa 252-5258, Japan
[2] TEP Co. Ltd, 2-20-4 Kosuge, Katsushika-ku, Tokyo 124-0001, Japan

E-mail: motoki@phys.aoyama.ac.jp

Received 15 October 2019, revised 23 December 2019
Accepted for publication 22 January 2020
Published 12 February 2020

Abstract

Since REBCO melt-textured bulks are produced in an extremely carrier underdoped state after melt-growth, oxygen-annealing is required for a few hundred hours to control the oxygen composition throughout the bulks due to their slow oxygen-diffusivity. In this study, we discovered that the oxygen-annealing time can be largely reduced with the introduction of water vapor to the oxygen-annealing process for Ag-added YBCO melt-textured bulks without any degradation of the superconducting properties. It was revealed that highly dense stacking faults were induced to the matrix during this wet oxygen-annealing, which are considered to act as fast diffusion paths of oxygen. The estimated chemical diffusion coefficients of oxygen at 400 °C for the bulk annealed under wet O_2 was $\sim 4.3 \times 10^{-11}$ $m^2 s^{-1}$, which is almost twice as high as that annealed under standard dry O_2 atmosphere. High J_c without a decrease in T_c was confirmed for the sample annealed under wet O_2, when the wet O_2 annealing was performed for a moderate time. In addition, a combined oxygen-annealing process, where wet O_2 was supplied for the first 24 h followed by a dry O_2 process for the remaining period, was found to be more effective to achieve both enhanced oxygen-diffusion and maintain high field trapping properties. These improvements are probably because moderate amounts of defects were introduced to the bulk as a function of the duration of the wet O_2 annealing. The introduction of water vapor to the oxygen-annealing process will become a versatile technique to reduce the total processing time of REBCO melt-textured bulks.

Keywords: REBCO, TSMG, melt-textured bulks, oxygen-diffusion, water vapor

(Some figures may appear in colour only in the online journal)

1. Introduction

Single-domain $REBa_2Cu_3O_y$ (REBCO, RE: rare earth element) melt-textured bulks have been widely studied for applications using their high critical current densities (J_c) and high field trapping properties. For example, REBCO bulks are developed for applications such as current leads, portable high-field magnets for medical devices, desktop NMR/MRI, superconducting motors, compact magnetic shielding systems and magnetically levitated bearings [1–6].

To achieve high field trapping properties, both enhancement of intergrain J_c and enlargement of size in bulks are important. Also, reinforcement of the bulk against hoop stress is necessary for high trapped field applications. Addition of silver (Ag) is one of the effective ways to fill voids which can trigger the destructive cracking inside the bulk

under high fields [7]. A very high maximum trapped field of more than 17 T below 30 K has been reported thus far for Ag-added REBCO bulks with additional reinforcements such as resin impregnation and stainless-steel enclosures [8, 9].

In all cases, the oxygenation process is indispensable for the as-synthesized REBCO materials to achieve a high critical temperature (T_c) of more than 90 K since REBCO has a large oxygen nonstoichiometry ($y = 6$–7) and REBCO is always in the carrier underdoped state after the crystal growth. Usually, oxygenation is conducted through post oxygen-annealing under a flowing O_2 atmosphere at around 300–500 °C depending on the rare earth elements in the REBCO. It is one of the major problems in REBCO melt-textured bulks that oxygen-annealing needs hundreds of hours due to the quite slow oxygen-diffusion in textured bulk materials under such annealing temperatures.

From the ideal diffusion equation, it is expected that the oxygen-diffusion time increases proportionaly to the square of the diameter of the bulks. However, most of the reported duration of the oxygen-annealing processes is in the range of 100–300 h with a weak correlation between the diameter of the bulk and the oxygen-annealing time. It is notable that it takes ~100 h to oxygenate a small piece of bulk with the size of ~1 mm^3. Diko *et al* reported that micro-cracks are induced during the oxygenation process with changes in the lattice constants, which plays a crucial role in shortening the oxygen-annealing time for large bulks [10]. Also, Yamada *et al* reported that the averaged chemical diffusion coefficients of oxygen at 400 °C are $\sim 1.0 \times 10^{-10}$ m^2s^{-1} and $\sim 5.0 \times 10^{-11}$ m^2s^{-1} for Ag-free and Ag-added YBCO melt-textured bulks, respectively [11]. Combined with the fact that the oxygen diffusion coefficients along the *ab*-plane at 400 °C for YBCO single crystals are reported to be in the order of 10^{-15} m^2s^{-1} [12], dispersed micro-cracks, voids and many other defects inside the bulks act as fast oxygen-diffusion paths in REBCO textured bulks. Meanwhile, our previous study revealed that reduction of voids through densification of the bulks resulted in improvement of J_c [13]. Therefore, longer oxygen-annealing should be needed when aiming for the preparation of high-performance bulks with high density.

In order to shorten the oxygenation time, we attempted to introduce additional diffusion paths in REBCO melt-textured bulks without degradation of the superconducting properties. There are some studies on the effects of heat-treatment including water vapor on REBCO single crystals, bulks and thin films mainly from the view of the evaluation of corrosion through reactions between REBCO and air components [14–17]. According to these studies, planar stacking faults at Cu-O chains are easily introduced by the heat-treatment containing water vapor. For example, Rupeng *et al* reported for YBCO polycrystalline sintered bulks that short-time exposure to 65 °C steam resulted in the generation of stacking faults [14]. Similar results have been reported for REBCO thin films by Günther *et al* where long-time annealing under water vapor induced the phase transition of REBCO crystal structures to $RE_2Ba_4Cu_7O_y$ (RE247) or $REBa_2Cu_4O_8$ (RE124) structures through the generation of dense stacking faults [15].

On the other hand, it has long been believed that water is poisonous to REBCO materials because corrosion deteriorates the superconducting properties. This is most likely when heat-treatment is conducted in air where CO_2 coexists or REBCO materials are subject to high partial pressure of water vapor such as an immersion in boiling water [16–19]. However, Bobylev *et al* reported for REBCO melt-textured bulks that flux pinning properties were improved by the introduction of planar stacking faults through annealing under oxygen or argon flows with water vapor (~0.2 wt% H_2O) which did not contain CO_2 [20].

Based on this background, we focused on the effects of introduced defects on oxygen-diffusivity in REBCO melt-textured bulks through oxygen-annealing in an atmostpher that is CO_2–free and containing water vapor in the present study.

2. Methods

A powder mixture consisting of Y_2O_3 (99.9%), $BaCO_3$ (99.9%) and CuO (99.9%) with the molar ratio of 1.3:1.7:2.4 was calcined twice in air at 880 °C for 12 h to obtain the precursor powder composed of YBCO and Y_2BaCuO_5 (Y211) with the molar ratio of 7:3. 10 wt% Ag_2O and 0.1 wt% Pt were added to the precursor in order to fill voids and to suppress the grain growth of Y211, respectively. Then the precursor was uniaxially pressed into disks 16 mm in diameter. Crystal-growth was carried out in air applying the top-seeded melt-growth (TSMG) method using a NdBCO single crystal as a seed. The temperature profile for melt-solidification is as follows. The pellets were heated to 900 °C in 1 h and held for 1 h, heated to 1040 °C in 1 h and held for 1 h, cooled to 990 °C in 1 h, then slowly cooled to 950 °C at a rate of 0.5 °C h^{-1} and finally cooled to room temperature in the muffle furnace. Three single-domain TSMG bulks with the size of ~13 mm in diameter and ~10 mm in height were successfully obtained. Hereafter these three bulks will be expressed as #1, #2 and #3. Next two types of oxygen-annealing, hereafter expressed as 'dry O_2 annealing' and 'wet O_2 annealing', were conducted to two of the YBCO TSMG bulks (#1 and #2) at 400 °C, separately, where the dry O_2 and wet O_2 annealing are oxygen-annealing without or with water vapor, respectively. In the wet O_2 annealing, water vapor with a partial H_2O pressure (P_{H2O}) of ~2 kPa was introduced to the O_2 gas-flow by bubbling the O_2 gas through a water bath at ~25 °C. Detailed procedures of the oxygen-annealing are as follows. Dry O_2 annealing was performed on bulk #1: first annealing for 30 min and then the mass of the bulk was measured, then further annealing for 60 min and another measurement of mass, and these procedures were repeated. Wet O_2 annealing was performed on bulk #2: first annealing for 10 min then a measurement of the mass, then annealing for a further 20 min and measurement of mass, and these procedures were repeated. These processes were continued until the saturation of an increase in mass of the bulks.

In addition, modified oxygen-annealing was applied to bulk #3, where annealing under wet O_2 was conducted for

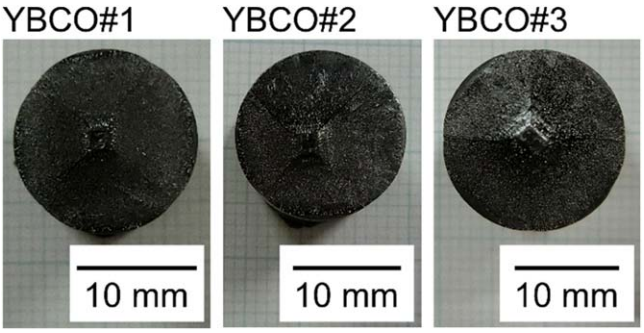

Figure 1. Appearance of the prepared three Ag-added YBCO TSMG bulks, #1, #2 and #3.

the first 24 h followed by annealing under dry O_2 up to 400 h. In all oxygenation processes, bulks were heated from room temperature to 400 °C in ~30 min in the tube furnace and furnace-cooled to room temperature. After the oxygenation of the bulks was completed, the highest trapped field was measured at 77 K using a Hall probe in contact with the polished surface of the bulks after magnetization using a permanent magnet of ~0.4 T.

Subsequently, All YBCO bulks were cut into pieces and their microstructures and superconducting properties were evaluated. Microstructures of the *ac*- and *ab*-planes of the bulks were observed using a 400 kV transmission electron microscope (TEM, JEOL JEM-4010). Magnetic susceptibility and magnetization hysteresis loops at 77 K and 40 K were measured for bulks #1 and #2 using a SQUID magnetometer (Quantum Design MPMS XL-5s) under dc fields up to 5 T. In these measurements, magnetic fields were always applied parallel to the *c*-axis of the pieces of the bulks. J_c values were calculated by means of the extended Bean model. After evaluation of the microstructures and superconducting properties, small rectangular pieces cut from bulks #1 and #2 were heated at 800 °C for 12 h in air in order to control the oxygen contents to be the underdoped state again. Then, J_c properties of these small pieces were evaluated successively as re-annealing under dry O_2 and wet O_2 at 400 °C was performed to the pieces of #1 and #2, respectively.

3. Results and discussion

The appearance of the as-grown three YBCO bulks, #1, #2 and #3, are shown in figure 1. All bulks are biaxially textured since four facet lines are clearly visible. At First, dry O_2 and wet O_2 annealing processes were applied to bulks #1 and #2, respectively, and changes in mass of the bulks with time were evaluated. Since oxygen-diffusion along the *c*-axis is negligible compared to diffusion in the *ab*-planes, the diffusion equation for the TSMG bulks is simplified to the oxygen-diffusion in an infinite cylinder by considering only the radial diffusion, where bulks are regarded as homogeneous cylinders. By giving proper initial and boundary conditions and adopting the approximations such that the oxygen-diffusion coefficient is unchanged regardless of oxygen compositions and that the oxygen compositional distribution inside the bulk

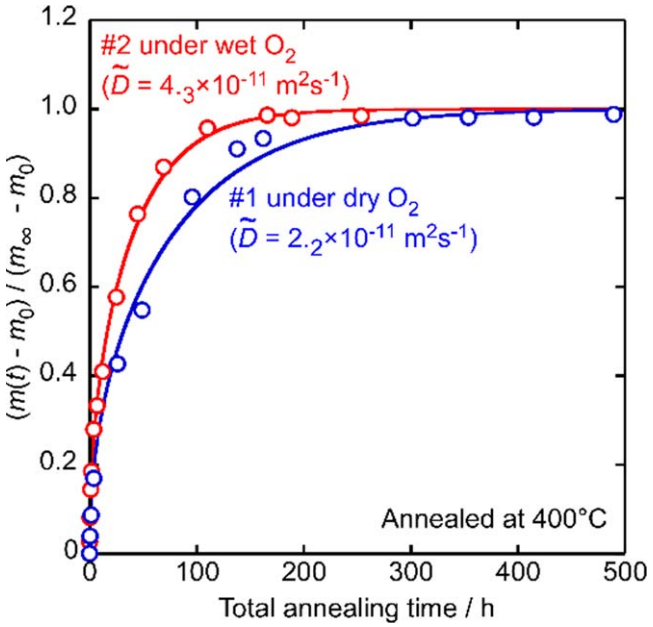

Figure 2. Total oxygen-annealing time dependences of mass-changes for Ag-added YBCO TSMG bulks annealed under dry O_2 and wet O_2 at 400 °C. The blue and red lines represent the least squared fitted curves using equation (2) for bulks #1 and #2, respectively.

is constant at the initial state, the diffusion equation can be analytically solved [21]. The time (t) dependence of oxygen compositions (C) at the distance r from the center of the bulk is expressed as equation (1), where r is in the range of 0 to the radius of the bulk (R). C_0, C_∞, $\tilde{D}$ and J_k ($k = 0, 1$) are oxygen compositions at the initial and equilibrium states, averaged chemical diffusion coefficients of oxygen and Bessel function of the first kind of order k, respectively. α_n is the nth root satisfying $J_0(\alpha_n) = 0$. By properly integrating equation (1), the time dependences of the mass of the bulks ($m(t)$) are derived as equation (2), where m_0 and m_∞ are the mass of the bulks at the initial and equilibrium states, respectively. From equation (2), the oxygen-diffusion coefficient, $\tilde{D}$, can be obtained as a fitting parameter by fitting the observed mass-changes with annealing-time by means of the least squared method.

$$\frac{C(r,t) - C_0}{C_\infty - C_0} = 1 - 2\sum_{n=1}^{\infty} \frac{\exp\left(-\alpha_n^2 \frac{\tilde{D}t}{R^2}\right) J_0\left(\alpha_n \frac{r}{R}\right)}{\alpha_n J_1(\alpha_n)} \quad (1)$$

$$\frac{m(t) - m_0}{m_\infty - m_0} = 1 - \sum_{n=1}^{\infty} \frac{4\exp\left(-\alpha_n^2 \frac{\tilde{D}t}{R^2}\right)}{\alpha_n^2} \quad (2)$$

Figure 2 shows the results of mass-changes and their fitting curves for the bulks annealed at 400 °C under dry O_2 for up to ~600 h and wet O_2 for up to ~250 h, respectively. The observed increase in mass after long-time annealing was ~1.3% under both annealing conditions, which corresponds to an increase in oxygen content y of $YBa_2Cu_3O_y$ of approximately ~0.78 given the compositions of TSMG bulks after melt-texturization, i.e. the molar ratio of YBCO, Y211, Ag and Pt, were the same as the nominal compositions. Assuming that each bulk reached the oxygen-equilibrium

state, $y \sim 6.93$, after long-time oxygen-annealing, the y value before annealing was estimated to be ~6.15. Equation (2) well fits the observed mass-changes although fittings are done without considering changes of the oxygen-diffusion coefficients as an increase in oxygen compositions y. An estimated oxygen-diffusion coefficient at 400 °C under wet O_2 annealing was $\sim 4.3 \times 10^{-11}$ m^2s^{-1} which was almost twice as high as that under dry O_2 annealing of $\sim 2.2 \times 10^{-11}$ m^2s^{-1}. Surprisingly, the introduction of water vapor to the oxygen-annealing process greatly enhances oxygen-diffusion in TSMG bulks.

After the series of oxygenation, bulks #1 and #2 exhibited maximum trapped fields of ~0.27 T and ~0.20 T at 77 K, respectively. It is considered that all annealed bulks do not include cracks nor chemical damages since the maximum trapped field of each bulk was detected almost at the center of the bulks. Although it may be a variation of the quality of each bulk, the slightly lower trapped field value for bulk #2 could be caused by some undesirable effects on J_c properties or grain-boundary characteristics after wet O_2 annealing for a long time, which will be discussed later.

We also evaluated the constituent phases of randomly oriented YBCO bulks before and after wet O_2 annealing at 400 °C for ~120 h. From powder x-ray diffraction measurements, peaks due to $Ba(OH)_2$ or $BaCO_3$ were not detected after wet O_2 annealing. It is considered that impurities such as $Ba(OH)_2$ and $BaCO_3$ are scarcely generated in TSMG bulks after long-time wet O_2 annealing.

Although dependences of P_{H2O} on oxygen-diffusivity for REBCO TSMG bulks have not been clarified yet, it is considered that oxygen-diffusion will advance faster as an increase in P_{H2O} based on our study about wet O_2 annealing on REBCO thin films where more stacking faults were introduced to the REBCO matrix as an increase in P_{H2O} [22].

After the series of oxygenation processes, the YBCO bulks annealed under dry O_2 and wet O_2, corresponding to #1 and #2, were cut into small rectangular pieces for microstructural observation and evaluation of superconducting properties. From secondary electron images of the polished surfaces of the two bulks (not shown), Ag was found to fill most of the large voids, especially close to the seed crystals. In addition, any noticeable differences such as the size and distribution of Y211 particles were not found between the two samples.

Figures 3(a) and (b) show the TEM images and selected area electron diffraction (SAED) patterns of the YBCO matrix for the bulks #1 and #2 after oxygenation, respectively. The observed positions are the c-growth region ~5 mm below the seed crystal. As for dry O_2 annealed bulks, a mostly homogeneous and defect-free matrix was observed although some defects existed in the regions around small precipitates such as Ag and Y211. On the other hand, highly dense stacking faults are observed throughout the observed regions for the wet O_2 annealed bulk, especially around the precipitates, which is due to the existence of water vapor during the annealing process.

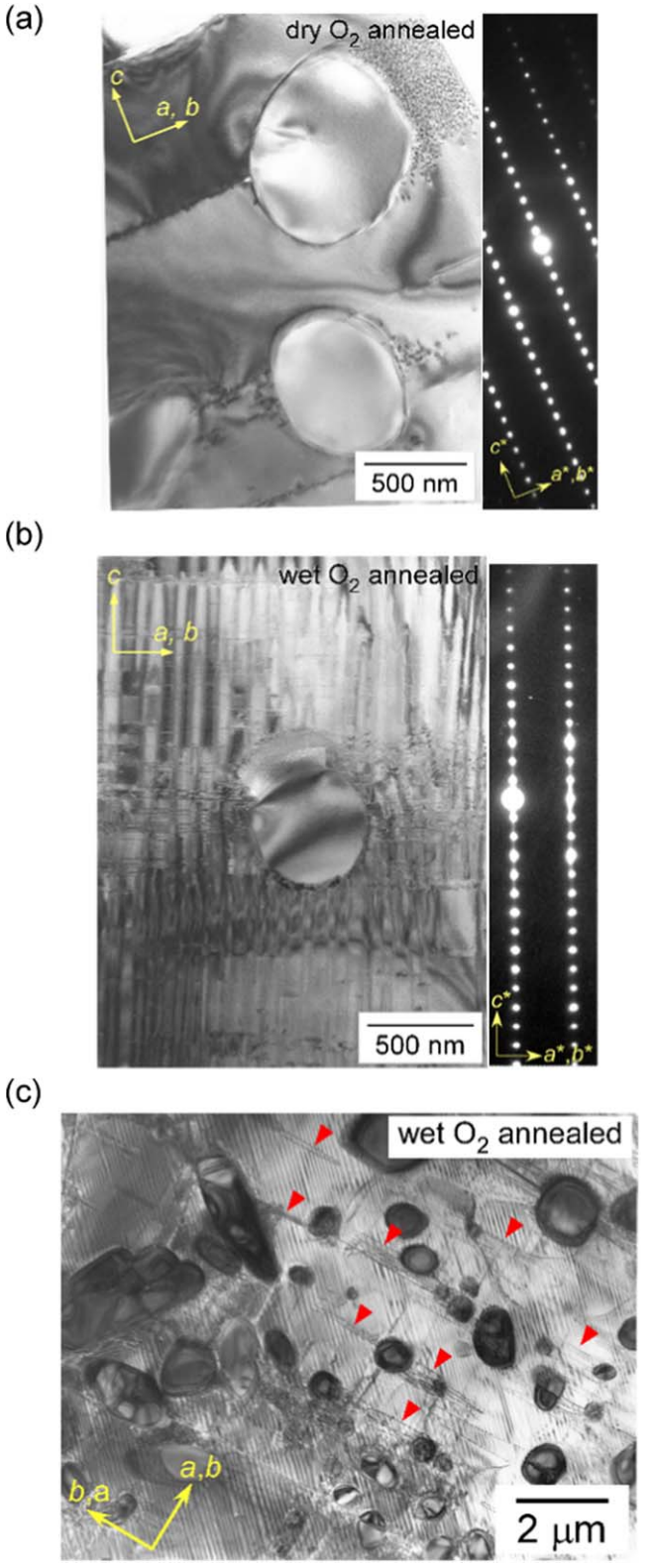

Figure 3. TEM images of the *ac*-planes with SAED patterns (a), (b) and the *ab*-plane in the *c*-growth region (c) for the bulks annealed under dry O_2 (a) and wet O_2 (b), (c). Highly dense stacking faults traveling along *ab*-planes are clearly visible for the sample annealed under wet O_2. Defects along the *a*-axis, shown with red arrows, were also observed only for the wet O_2 annealed sample.

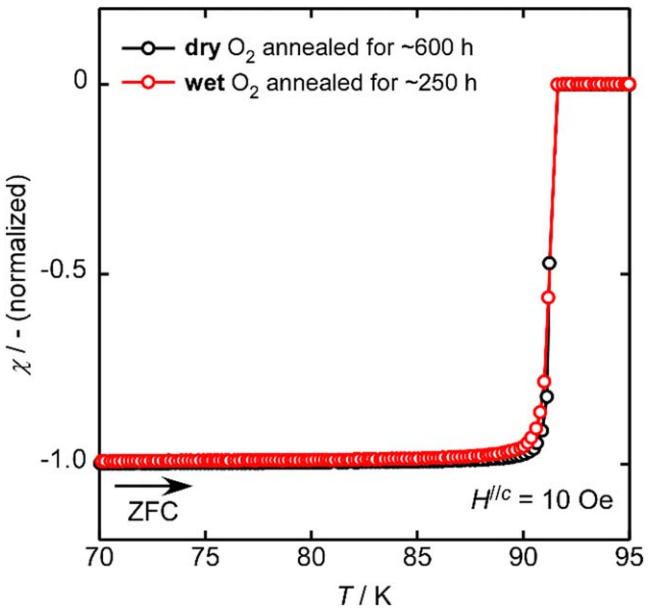

Figure 4. Temperature dependences of ZFC magnetization for pieces cut from bulks annealed under dry O_2 or wet O_2 for a long time.

Streaks along the c^*-direction are observed in SAED patterns of the wet O_2 annealed bulks, which also demonstrates the existence of dense planar defects. These kinds of streaks are also reported for REBCO films with dense stacking faults [23, 24]. In addition, twin boundaries shown as vertical stripes are observed with intervals of less than 100 nm in this observed region. Figure 3(c) shows a planar TEM image of the *ab*-plane of the wet O_2 annealed sample. [110] directed twin structures are clearly visible. In addition to the twin boundaries, a lot of thin defects which are in parallel along the *a*-axis direction of the YBCO crystal (shown by red arrows) are observed around the precipitates only for a wet O_2 annealed sample. Although the detailed morphology and generation-mechanism of these defects have not been clarified at this moment, some possibilities are that the observed specimens were slightly tilted so that planar stacking faults in the *ab*-plane became visible or that other kinds of planar defects were induced owing to distortions or internal stresses around the precipitates through wet O_2 annealing. From the above observation and the estimated oxygen-diffusion coefficients, it can be concluded that dense planar faults effectively act as fast oxygen-diffusion paths for Ag-added YBCO TSMG bulks.

The superconducting properties were then evaluated for the small pieces with the size of $\sim 1.2 \times 0.6 \times 0.6^{//c}$ mm^3 in the *c*-growth region ~4 mm below the seed crystal. Hereafter, these small pieces cut from bulks #1 and #2 annealed for a long time will be expressed as pc_#1_ox and pc_#2_ox, respectively. Figure 4 shows the temperature dependences of the zero-field-cooled (ZFC) magnetization, χ, for pc_#1_ox and pc_#2_ox. Sharp superconducting transitions at ~91 K were observed for both samples. It was revealed that the existence of water vapor during the oxygenation process does not degrade T_c.

In order to clarify the changes of the superconducting properties of the bulks with oxygen-annealing time, pc_#1_ox and pc_#2_ox were heated at 800 °C for 12 h in air to control the oxygen composition to be the underdoped state. These reductive-annealed samples will be expressed as pc_#1_red and pc_#2_red, respectively. Then, oxygen-annealing under dry O_2 and wet O_2 at 400 °C was separately performed to pc_#1_red and pc_#2_red. Figures 5(a) and (b) show the changes in T_c^{onset}, T_c^{mid} and T_c^{end} with annealing time for pc_#1_red and pc_#2_red, respectively. T_c^{onset}, T_c^{mid} and T_c^{end} are defined such that normalized magnetizations are equal to −0.05, −0.50 and −0.95, respectively. Dashed lines represent the T_c^{onset}, T_c^{mid} and T_c^{end} of pc_#1_ox and pc_#2_ox. From figure 5(a), it takes more than 30 h to recover sharp superconducting transitions under dry O_2, whereas annealing for only ~10 h is enough under wet O_2 as shown in figure 5(b). It was also revealed for small pieces that introduction of water vapor is especially effective to promote oxygen-diffusion. It should be noted that oxygenation for both samples proceeded quite rapidly under the second oxygen-annealing, which is probably because microcracks were induced during the first oxygenation and/or following reductive heat-treatment at 800 °C.

Figure 6 shows the J_c-H curves at 77 K and 40 K for pc_#1_ox and pc_#2_ox (shown as open symbols), and pc_#2_red after successive addition of annealing at 400 °C under wet O_2 (shown as closed symbols). At first, by comparing the two pieces, pc_#1_ox and pc_#2_ox, annealed for a long time, pc_#2_ox showed decreased in-field J_c, which is probably due to a decrease in superconducting condensation energy by the introduction of excessive amounts of defects such as stacking faults to the YBCO matrix. These results are consistent with the decreased trapped field for the wet O_2 annealed bulk #2 mentioned before. However, after high-temperature heat-treatment at 800 °C followed by successive addition of wet O_2 annealing, the in-field J_c was higher than that of pc_#2_ox. The best J_c properties were observed for pc_#2_red after wet O_2 annealing for only 5 h, shown as red closed symbols, whose properties were almost comparable to those of pc_#1_ox, shown as black open symbols. It should be noted that the J_c-H properties gradually decrease with increases in annealing-time under wet O_2 after annealing for 5 h. As for the pc_#1_red (not shown), although J_c gradually recovered toward that of pc_#1_ox with an increase in annealing-time under dry O_2, an annealing duration of up to ~48 h was still insufficient. From the above results, it is considered that existence of water vapor during the annealing process largely shortens oxygenation-time without any negative influence on superconducting properties, as long as the duration of the wet O_2 annealing is properly regulated.

Considering the above discussion, although the introduction of water vapor to the annealing process greatly promotes oxygen-diffusion, excessive long-time annealing under wet O_2 will result in deterioration of J_c properties, probably due to the introduction of excessive defects to the YBCO matrix. Therefore, the effects of a modified oxygen-annealing consisting of wet O_2 and dry O_2 processes were investigated for an Ag-added YBCO TSMG bulk #3, where wet O_2 annealing was applied for the first 24 h followed by the standard dry O_2 annealing for up to ~400 h. It should be

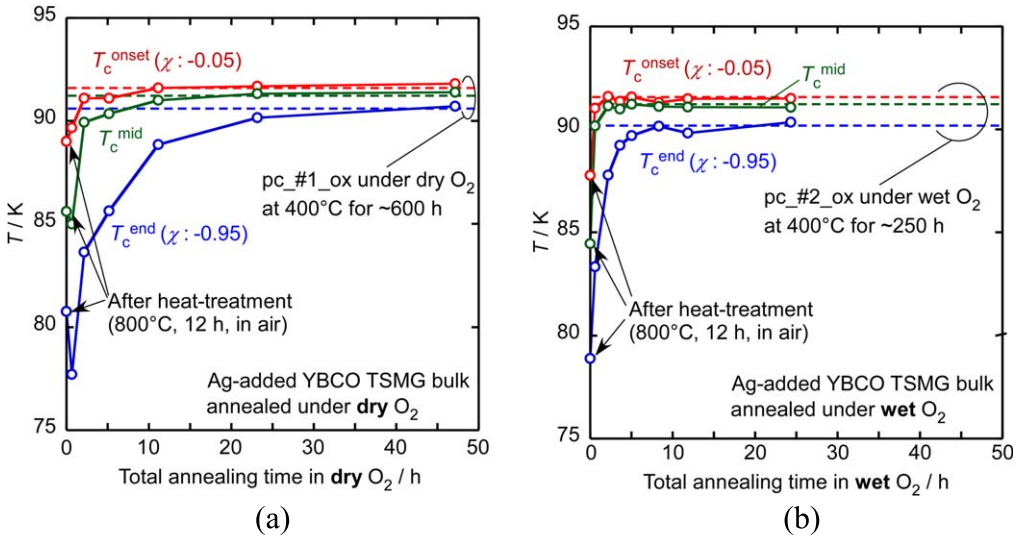

Figure 5. Changes in T_c^{onset}, T_c^{mid} and T_c^{end} with annealing-time for the pieces of the Ag-added YBCO TSMG bulks after heat-treatment at 800 °C for 12 h in air, pc_#1_red and pc_#2_red, followed by successive addition of annealing at 400 °C under dry O_2 (a) and wet O_2 (b), respectively. The dashed lines represent T_c^{onset}, T_c^{mid} and T_c^{end} of pc_#1_ox (a) and pc_#2_ox (b).

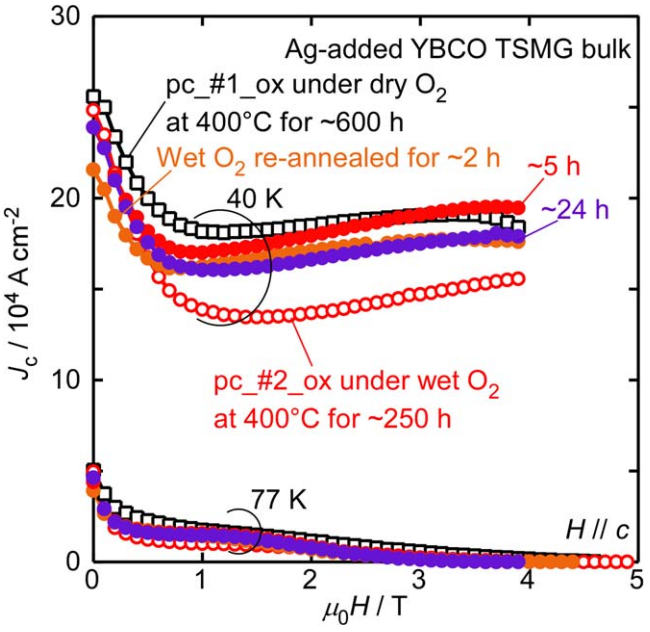

Figure 6. J_c–H curves at 77 K and 40 K for pc_#1_ox and pc_#2_ox (open symbols) and pc_#2_red after successive addition of annealing at 400 °C under wet O_2 (closed symbols). Total oxygen-annealing times are indicated in the figure.

noted that the mass of the bulk was almost unchanged after dry O_2 annealing for ~300 h. An averaged chemical diffusion coefficient of oxygen, $\tilde{D}$, of the bulk #3 was estimated to be $\sim 2.7 \times 10^{-11}$ m^{2}s^{-1} from the same fitting mentioned before, whose value is in the range between those of the bulks annealed under dry O_2 and wet O_2. This modified annealed bulk #3 showed the maximum trapped field at 77 K of 0.26 T, which is almost equivalent to that of the bulk #1 annealed only under dry O_2 for a long time.

After completion of the modified oxygen-annealing, bulk #3 was cut into pieces for microstructural observation. Figures 7(a) and (b) show the TEM images of the *ac*-plane

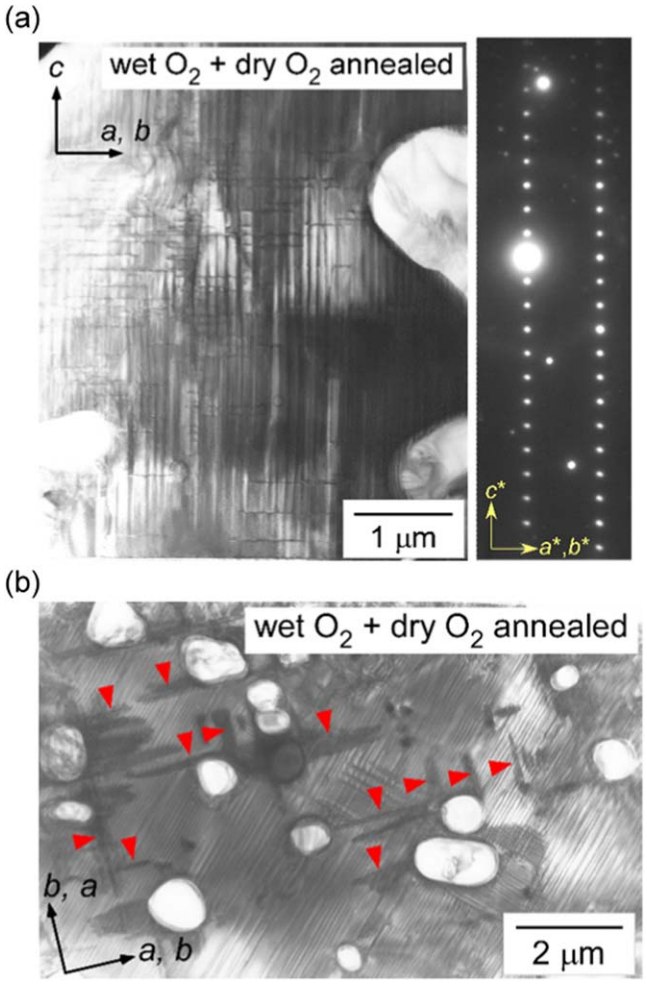

Figure 7. TEM images of the *ac*-plane with SAED patterns (a) and the *ab*-plane in the *c*-growth region (b) for the bulk #3 annealed under wet O_2 for 24 h followed by dry O_2 for ~400 h. Stacking faults traveling along the *ab*-planes are clearly visible (a). Contrasted regions along *a* or *b*-axes as shown by red arrows were also observed (b).

Table 1. Summary of the oxygen-annealing conditions, estimated oxygen-diffusion coefficients at 400 °C and maximum trapped fields at 77 K for Ag-added YBCO TSMG bulks.

	Oxygen-annealing condition at 400 °C	$\tilde{D}$(400 °C)/10^{-11} m^2s^{-1}	Maximum trapped field at 77 K/ T^{-1}
YBCO #1	Dry O_2	$2._2$	0.27
YBCO #2	Wet O_2	$4._3$	0.20
YBCO #3	Wet O_2 (24 h) + Dry O_2	$2._7$	0.26

with SAED patterns and the *ab*-plane of bulk #3, respectively. The observed positions are the *c*-growth region ~5 mm below the seed crystal. From the *ac*-plane microstructure, a number of stacking faults are clearly visible. However, in the case of the modified annealed samples, streaks along the c^*-direction are not observed in the SAED patterns, which suggests that bulk #3 has a lower density of stacking faults than that of bulk #2 annealed only under wet O_2 for a long time as shown in figure 3(b). In addition, dark gray regions around the precipitates as well as twin boundaries were clearly observed in the *ab*-plane of bulk #3. From the above results, it is considered that planar faults can be controllably introduced as a function of the duration of wet O_2 annealing.

Table 1 summarizes the annealing conditions, estimated chemical diffusion coefficients of oxygen and the maximum trapped fields at 77 K for the Ag-added YBCO TSMG bulks in this study. Through optimization of the oxygen-annealing consisting of wet O_2 and dry O_2 processes, it is possible to reduce the oxygen-annealing time without degrading the high field trapping properties of the bulks.

We also confirmed that wet O_2 annealing is effective to shorten the annealing-time for Ag-free YBCO and DyBCO TSMG bulks, which will be reported elsewhere. It is expected that this technique will be more effective for other REBCO materials with light rare earth elements which require lower oxygen-annealing temperatures of ~300 °C, where diffusion of oxygen is much slower to reach an optimally doped state of the carrier. Introduction of water vapor to the oxygen-annealing process will become a versatile technique to reduce the total oxygenation processes.

4. Conclusion

In order to reduce total oxygenation processes for REBCO melt-textured bulks, oxygen-annealing containing water vapor was investigated for Ag-added YBCO TSMG bulks. The estimated chemical diffusion coefficients of oxygen at 400 °C for the bulk annealed under wet O_2 was $\sim 4._3 \times 10^{-11}$ m^2s^{-1}, whose value was almost twice as high as that annealed under a standard dry O_2 atmosphere. It was revealed from the microstructural observation that highly dense planar faults parallel to the *ab*-direction were induced through wet O_2 annealing. These planar faults are considered to act as effective oxygen-diffusion paths. From the evaluation of the superconducting properties for small pieces cut from the bulks, there was no degradation of T_c after long-time annealing under wet O_2. It was reproducibly confirmed for both large and small samples that annealing under wet O_2 greatly enhances oxygen-diffusion. In addition, high in-field J_c was achieved for the sample annealed under wet O_2 for ~5 h, which was almost comparable to that annealed under standard dry O_2 for a much longer time. However, in-field J_c gradually degraded with an increase in annealing-time under wet O_2 for more than 5 h, probably due to a decrease in superconducting condensation energy following the introduction of excessive amounts of defects such as stacking faults to the YBCO matrix. Finally, the effects of a combined oxygen-annealing method consisting of both wet O_2 and dry O_2 processes was investigated. Through this modified annealing, enhanced diffusion of oxygen was achieved without any degradation of field trapping properties probably because moderate amounts of defects were controllably introduced to the bulk. Introduction of water vapor to the oxygen-annealing process will become a versatile technique to reduce the total oxygenation processes. It is expected that this technique can be extended to other REBCO materials with light rare earth elements such as SmBCO, EuBCO and GdBCO which require lower oxygen-annealing temperatures where the diffusion of oxygen is much slower to reach an optimally doped state of the carrier.

Acknowledgments

This work was supported by the JSPS KAKENHI, grant number 19K05006, Japan. The TEM observation in this work was supported by Center for Instrumental Analysis, College of Science and Engineering, Aoyama Gakuin University.

ORCID iDs

T Motoki https://orcid.org/0000-0003-3218-0977

References

[1] Durrell J H, Ainslie M D, Zhou D, Vanderbemden P, Bradshaw T, Speller S, Filipenko M and Cardwell D A 2018 *Supercond. Sci. Technol.* **31** 103501
[2] Teshima H, Sawamura M and Hirano H 2002 *Physica* C **378–381** 827–32
[3] Solovyov M, Souc J, Gomory F, Rikel M O, Mikulasova E, Usakova M and Usak E 2017 *IEEE Trans. Appl. Supercond.* **27** 2–5
[4] Iwakuma M, Hase Y, Satou T, Tomioka A, Konno M, Iijima Y, Saitoh T, Yamada Y, Izumi T and Shiohara Y 2009 *IEEE Trans. Appl. Supercond.* **19** 1648–51
[5] Nakamura T, Tamada D, Yanagi Y, Itoh Y, Nemoto T, Utumi H and Kose K 2015 *J. Magn. Reson.* **259** 68–75

[6] Werfel F N, Floegel-Delor U, Rothfeld R, Riedel T, Goebel B, Wippich D and Schirrmeister P 2012 *Supercond. Sci. Technol.* **25** 014007
[7] Yeh F and White K W 1991 *J. Appl. Phys.* **70** 4989–94
[8] Tomita M and Murakami M 2003 *Nature* **421** 517–20
[9] Durrell J H *et al* 2014 *Supercond. Sci. Technol.* **27** 082001
[10] Diko P, Granados X, Bozzo B and Kulík P 2007 *IEEE Trans. Appl. Supercond.* **17** 2961–4
[11] Yamada T, Ikuta H, Yoshikawa M, Yanagi Y, Itoh Y, Oka T and Mizutani U 2002 *Physica* C **378–381** 713–7
[12] Tsukui S, Adachi S, Oshima R, Nakajima H, Toujou F, Tsukamoto K and Tabata T 2001 *Physica* C **351** 357–62
[13] Setoyama Y, Shimoyama J I, Motoki T, Kishio K, Awaji S, Kon K, Ichikawa N, Inamori S and Naito K 2016 *Physica* C **531** 79–84
[14] Rupeng Z, Goringe M J, Myhra S and Turner P S 1992 *Philos. Mag.* A **66** 491–506
[15] Günther W, Schöllhorn R, Siegle H and Thomsen C 1996 *Solid State Ionics* **84** 23–32
[16] Regier M, Keskin E and Halbritter J 1999 *IEEE Trans. Appl. Supercond.* **9** 2375–9
[17] Roa J J, Jiménez-Piqué E, Díaz J, Morales M, Calleja A and Segarra M 2012 *Surf. Coatings Technol.* **206** 4256–61
[18] Diko P, Piovarči S, Antal V, Kaňuchová M and Volochová D 2018 *J. Am. Ceram. Soc.* **101** 3703–9
[19] Nariki S and Murakami M 2002 *Physica* C **378–381** 769–73
[20] Bobylev I B, Gerasimov E G and Zyuzeva N A 2015 *Cryogenics* **72** 36–43
[21] Crank J 1975 *The Mathematics of Diffusion* (Oxford: Clarendon)
[22] Gondo S, Motoki T and Shimoyama J 2020 in preparation
[23] Anand S and Srivastava O N 2004 *Bull. Mater. Sci.* **27** 113–9
[24] Aytug T *et al* 2005 *J. Appl. Phys.* **98** 2–7